IEEE Photonics Journal
An IEEE Photonics Society Publication

Polarization-Independent Filter Based on 2-D Crossed Grating Under Oblique Incidence

Volume 10, Number 5, September 2018

Danyan Wang, *Student Member, IEEE*
Qingkang Wang
Zhongqiu Zhan

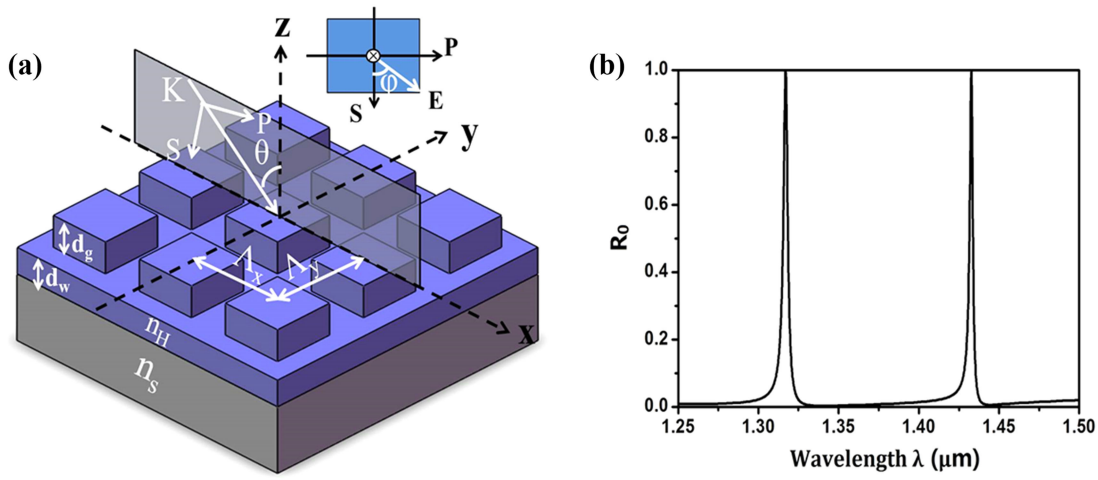

DOI: 10.1109/JPHOT.2018.2868432
1943-0655 © 2018 IEEE

Polarization-Independent Filter Based on 2-D Crossed Grating Under Oblique Incidence

Danyan Wang, *Student Member, IEEE*, Qingkang Wang, and Zhongqiu Zhan

The Key Laboratory for Thin Film and Microfabrication Technology of Ministry of Education, School of Electronic Information and Electrical Engineering, Shanghai Jiao Tong University, Shanghai 200240, China

DOI:10.1109/JPHOT.2018.2868432

Manuscript received August 13, 2018; accepted August 27, 2018. Date of publication September 17, 2018; date of current version September 26, 2018. This work was supported by National High-Tech Research and Development Program of China State 863 Projects under Grant 2011AA050518. Corresponding author: Qingkang Wang (e-mail: wangqingkang@sjtu.edu.cn).

Abstract: The existing polarization-insensitive filters based on two dimensional (2-D) grating are mostly under normal incidence. However, in filtering optical devices, the normal incidence regime is usually avoided because it requires the use of beam separators which yields a loss of efficiency. Herein, we present a compact method to realize polarization-independent filter under oblique incidence, which is implemented on 2-D crossed grating in the telecommunication region. Plane of incidence is set to be in *xz* plane and three different polarization angles (0°, 45°, and 90°) are used to demonstrate the polarization-insensitivity. Realization of the polarization-insensitivity of the 2-D filter is based on the split feature under oblique incidence, according to the analysis of the physical mechanism. The location of the polarization-independent resonance is mainly determined by the grating period along x-axis and will right shift with increasing the period. Results show that the polarization-insensitive resonances occur at 1356.9 nm, 1372.6 nm and 1398.5 nm when the grating periods along x-axis are 830 nm, 850 nm and 870 nm, respectively. Moreover, the results and methods provided herein can be applied to search for the polarization-insensitive resonances of the 2-D grating with other planes of incidence.

Index Terms: Guided mode resonant filter (GMRF), 2-D grating, rigorous coupled wave analysis (RCWA), polarization-independent filter.

1. Introduction

Resonant gratings offer a simple structure with a minimal number of layers, which have a rich variety of applications such as optical filters [1], [2], photonics detectors [3], sensors [4], and switch devices [5], etc. Among the numerous applications, guided mode resonant filter (GMRF) which incorporates resonant coupling to leaky Bloch modes in the waveguide-grating layer system has drawn much attention recently, because of its high diffraction efficiency, narrow band, spectral or color sensitivity, etc. [6]–[8], [27]. Unfortunately, the resonant peaks are inevitably susceptible to incident polarization, which affect the performances for certain applications such as dense wavelength division multiplexing [9] and laser devices [10].

There have been a variety of designs proposed to realize polarization-insensitive filters based on 1D GMRF for both normal and oblique incidences. Muhammad *et al.* reported two types of

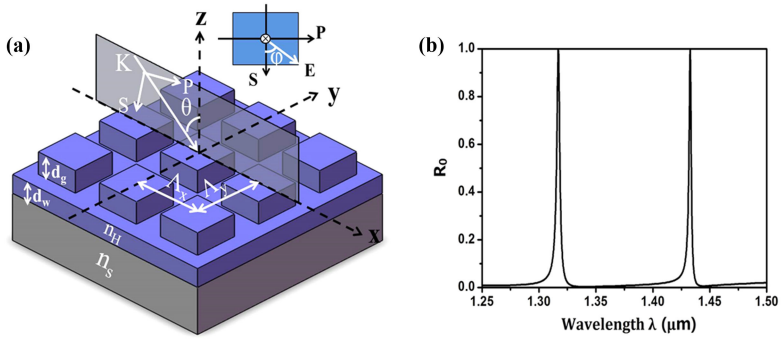

Fig. 1. (a) Schematic structure of the designed 2D GMRF. d_g is the grating thickness, d_w is the waveguide layer thickness, Λ_x and Λ_y are grating periods along x- and y-axis with f Λ_x and fΛ_y being the corresponding widths. Plane of incidence is set to be in xz-plane in order to simplify the analysis process. (b) The target zero-order reflectance spectra (R_0) of designed 2D GMRF under normal incidence. And the optimized structure parameters are: $\Lambda_x = \Lambda_y = 850$ nm, f = 0.38, $d_g = 350$ nm, $d_w = 330$ nm. In addition, $n_s = 1.4$, $n_H = 2.0$, $n_c = 1.0$, $\theta = \varphi = 0^\circ$.

non-polarizing resonant filters based on 1D GMRF with classic mounting under normal incidence [11], [12]. G. Niederer, D. Lacour and B. Xu *et al.* designed and characterized a type of polarization-independent resonant grating filter with full conical mounting under normal incidence, respectively [13]–[15]. For oblique incidence, X. Hu *et al.* reported a theoretical non-polarization filter at oblique incidence in the infrared range [16]. X. M. Gao *et al.* presented an angular-dependent polarization-insensitive filter fashioned with zero-contrast grating under classic mounting [17]. Furthermore, D. Wang *et al.* reported a polarization insensitive filter based on 1D grating under oblique incidence with plane of incidence between classic and conical mountings [18].

As for the GMRF structure with 2D grating, the reported researches about polarization independency were mainly concentrated on normal incidence [19]–[22], [26], [28]. However, in filtering optical devices, the normal incidence regime is usually avoided because it requires the use of beam separators which yields a loss of efficiency. Up to now, to the author's knowledge, only a few researches have been carried out on polarization-independent GMRF, which was implemented on 2D gratings under oblique incidence. For example, Fehrembach *et al.* succeeded in obtaining narrow-band unpolarized filters in 2005 [23], 2008 [24] and 2010 [25], respectively. However, the methods proposed by Fehrembach were based on the analysis of the electric field, which was a little esoteric and difficult to understand.

In this paper, we present a compact method to realize the polarization-insensitivity of 2D GMRF with crossed pillars under oblique incidence, which is based on its split features. Plane of incidence (POI) is set to be in xz-plane and three incident polarization states ($\varphi = 0^\circ$, 45°, 90°) are used to demonstrate the polarization-independency. Moreover, the results and methods provided here can be applied to the 2D GMRF under other planes of incidences.

2. Structure and Design Methods

Fig. 1(a) illustrates the proposed structure, which consists of a 2D crossed diffraction grating with rectangular pillars, a waveguide layer and a substrate. Λ_x and Λ_y are grating periods along x- and y-axis with fΛ_x and fΛ_y showing the corresponding grating widths. d_g and d_w are thicknesses of the grating layer and waveguide layer, respectively. The incident medium is assumed to be air in this paper, with refractive index n_c ($n_c = 1.0$). In addition, n_H ($n_H = 2.0$) and n_S ($n_S = 1.4$) are refractive indices of the thin films (grating layer and waveguide layer) and substrate, respectively. For simplicity, POI is set to be in xz-plane with wave vector K lying in this plane. Polarization of the E vector is oriented in a polarization plane normal to the direction defined by K, where $\varphi = 0^\circ$ corresponds to the S-polarization and $\varphi = 90^\circ$ is P-polarization. For S-polarized incidence, the E vector is perpendicular to the POI, while the E vector is parallel to the POI for incidence with

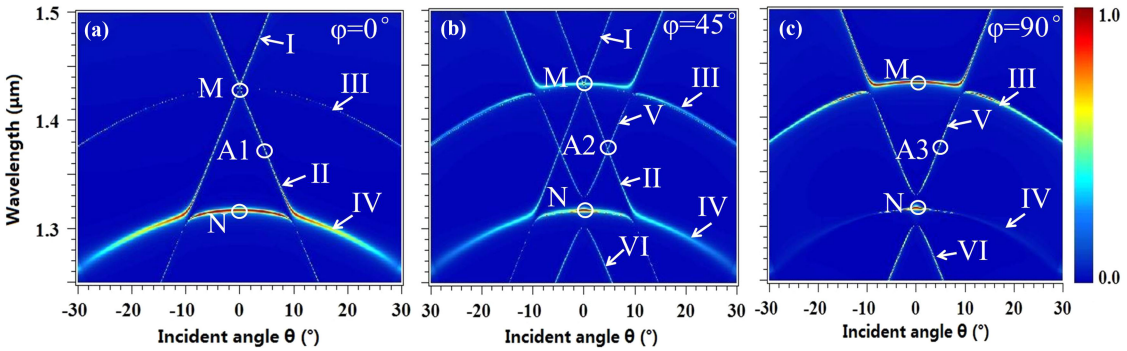

Fig. 2. Calculated results of angular-resolved reflectance (R_0) of the designed 2D filter with square pillars ($\Lambda_x = \Lambda_y = 850$ nm) under three different polarization states. (a) $\varphi = 0°$ (S-polarization); (b) $\varphi = 45°$; (c) $\varphi = 90°$ (P-polarization).

P-polarization. θ is the incident angle measured from z-axis in the plane of incidence. Besides, the wavelength is much larger compared with the grating period, e.g., in the subwavelength regime, so that only the zero-th diffraction order can propagate freely, while other higher orders are all evanescent.

Particle swarm optimization (PSO) combined with rigorous coupled wave analysis (RCWA) method is applied to design and optimize the 2D GMRF [26]. The grating periods Λ_x and Λ_y (here $\Lambda_x = \Lambda_y$), grating layer thickness d_g, waveguide layer thickness d_w and grating layer fill factor f are the optimization parameters. In addition, $n_s = 1.4$, $n_H = 2.0$, $n_c = 1.0$ and $\theta = \varphi = 0°$ during the optimization process. The FF is an rms error function:

$$FF = \left\{ \frac{1}{M} \sum_{\lambda_i} \left[R_{m,n}^{desired}(\lambda\lambda - R_{m,n}^{design})\lambda\lambda \right] \right\}^{1/2} \quad (1)$$

Where $R_{m,n}^{desired}(\lambda)$ is the desired set of total reflection diffraction efficiency and $R_{m,n}^{design}(\lambda)$ is its designed counterpart by PSO as well as RCWA method. Both *m* and *n*, which are the diffraction order numbers in the *x* and *y* directions, are equal to zero because of the subwavelength regime. M is the number of wavelength points. Commercially available software based on RCWA is used to further optimize the 2D structure as well as to perform the reflectance spectra. Fig. 1(b) shows the target zero-order reflectance (R_0) of the 2D GMRF under normal incidence, and in order to obtain the target response spectra under normal incidence the optimized structural parameters are: $\{\Lambda_x = \Lambda_y = 850\,\text{nm}, f = 0.38, d_g = 350\,\text{nm}, d_w = 330\,\text{nm}\}$. There are two resonances with wavelengths 1.317 μm and 1.433 μm, as illustrated in Fig. 1(b), because of the double periodicity. Moreover, the reflectance spectra of the designed structure exhibit high diffraction efficiency in the resonant peaks, low diffraction efficiency in sideband and narrow linewidth. Besides, the results also illustrate that, for an S-polarized beam ($\varphi = 0°$), the calculated zero-order reflectance (R_0) of the 2D GMRF under normal incidence shows a polarization-insensitivity compared to that for a P-polarized incidence ($\varphi = 90°$) because of the structural symmetry. However, there exists no symmetry of the 2D GMRF structure under oblique incidence. Therefore, we need to find the polarization-insensitive points under oblique incidence, which are obtained under several different polarization angles, as reported in Refs. [17], [18].

3. Results and Analysis

Fig. 2 shows the calculated reflection spectra (R_0) of the designed 2D GMRF with square pillars ($\Lambda_x = \Lambda_y = 850$ nm) versus the wavelength and incident angle. The incidences are ranging from $-30°$ to $30°$ and the wavelengths are in the telecommunication region from 1.25 μm to 1.5 μm. Dark blue represents the regions with low reflectivity, whereas dark red denotes those with high

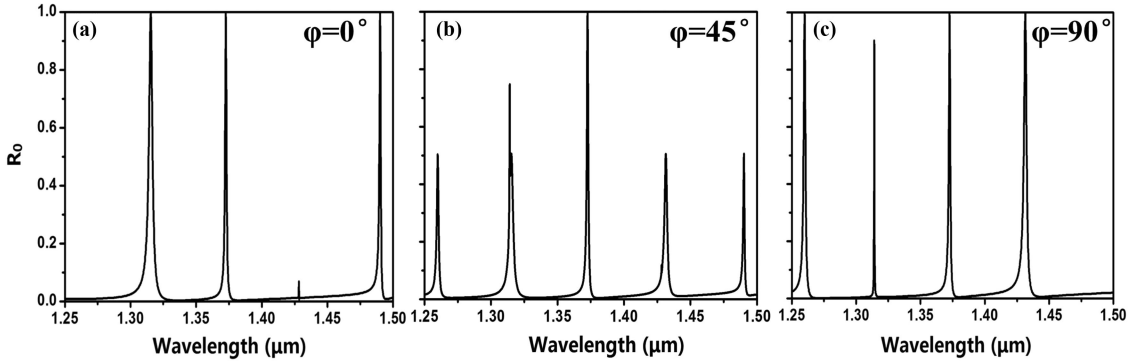

Fig. 3. Reflectance spectra of the designed 2D GMRF with square pillars ($\Lambda_x = \Lambda_y = 850$ nm) under oblique incidence $\theta = 4.7°$ with three different polarization angles. (a) $\varphi = 0°$; (b) $\varphi = 45°$; (c) $\varphi = 90°$.

reflectivity, as shown in the right color bar. Here, we only treat the positive incident angles because of the angle symmetry.

Take an S-polarized incidence ($\varphi = 0°$) for example, as shown in Fig. 2(a), there exist two pairs of resonance bands. One pair of them (branches I and II) are split from a fixed point M, whereas the other pair of them (branches III and IV) are all degenerated and they never split even under oblique incidence. While for P-polarized incidence ($\varphi = 90°$), as shown in Fig. 2(c), the calculated reflectance spectra of the 2D GMRF also exhibit two pairs of branches, where one pair of them (branches V and VI) are split from point N, and the other pair (branches III and IV) are also degenerate. The coordinates of the fixed points M and N are (0, 1.433) and (0, 1.317), respectively. That means the resonant locations of the 2D GMRF under normal incidence are 1.433 μm and 1.317 μm, which is in accordance with the designed reflectance spectra illustrated in Fig. 1(b). The difference between the split branches I, II in Fig. 2(a) and split branches V, VI in Fig. 2(c) is caused by the different eigenfunctions. Varying the polarization angle φ by a step of 45°, the angular-resolved reflectance of the 2D GMRF with an intermediate polarization angle are shown in Fig. 2(b). The spectra has clearly revealed that there are two pairs of split branches (I, II, V, VI) which are composing from the superposition of Fig. 2(a) and 2(c). Moreover, the other two branches III and IV are still degenerate and are consistent with those in Fig. 2(a) and 2(c). In addition, varying φ from 0° to 90° can generate a continuously diffraction efficiency transition from Fig. 2(a) to Fig. 2(c). During this continuously transition, there exists a distinct crossing point labeled as A2, which can be easily obtained from Fig. 2(b). Coordinate of the crossing point is (4.7, 1.3726), which means that the resonant wavelength is 1.3726 μm with an oblique incidence $\theta = 4.7°$. Besides, coordinate (4.7, 1.3726) also exists under S- and P-polarized incidences, as shown in Figs. 2(a) and 2(c) which marched as A1 and A3, respectively. Therefore, (4.7, 1.3726) is the polarization independent point that we are looking for. In order to understand clearly the polarization insensitivity, the reflection spectra of the point (4.7, 1.3726), under three different polarization angles as 0°, 45° and 90°, will be analyzed in detail in the following.

Fig. 3 illustrates the spectral reflectivity of the designed 2D GMRF under oblique incidence with $\theta = 4.7°$. In order to demonstrate the polarization-insensitivity, three different polarization angles ($\varphi = 0°$, 45° and 90°) are used to obtain the spectral reflectance. Results show that there are four resonances of the designed 2D GMRF under S-polarized ($\varphi = 0°$) and P-polarized ($\varphi = 90°$) incidences, as shown in Fig. 3(a) and 3(c), and there are five resonances of the 2D GMRF under polarization angles with $\varphi = 45°$, as exhibited in Fig. 3(b). Among them, the reflectance spectrum with wavelength 1.3726 μm exhibits high diffraction efficiency, narrow band and low sideband, etc. What's more important, the resonant location with wavelength 1.3726 μm is proved to be insensitive to polarization under oblique incidence of 4.7°.

The resonant locations of the two resonances with wavelengths 1315.4 nm and 1431.5 nm, which are near 1.317 μm, 1.433 μm, are polarization independent, as illustrated in Fig. 3(a), 3(b)

and 3(c). However, the diffraction efficiency of the resonance with wavelength 1315.4 nm is about 100% with $\varphi = 0°$, and becomes 50.6% and 90.2% with $\varphi = 45°$ and $\varphi = 90°$, respectively. And the diffraction efficiencies of the resonance with wavelength 1431.5 nm are about 1.3%, 50.6% and 100% with $\varphi = 0°$, 45° and 90°, respectively. Thus, the diffraction efficiencies of the two resonances are polarization-dependent and can be well applied to intensity-tunable filters. Furthermore, the two resonances belong to the resonant branches III and IV, as shown in Fig. 2. And as θ increases from 0°, branches III and IV present an excellent stability in its resonant locations. Therefore, the two resonances are also insensitive to oblique incidences.

Well known for that there are two branches of the 1D GMRF for a classic mounting under oblique incidence, which are split from a central resonant wavelength [17]. And there exist a pair of resonance bands of the 1D GMRF for a full conical mounting under oblique incidence, which are degenerate and never split no matter what the incident angle is [29]. For classic mounting, the incident plane is perpendicular to the grating grooves, and the incident plane is parallel to the linear bars for full conical mounting. For 2D GMRF with POI in xz-plane as presented in Fig. 1(a), the grating pillars along x-axis (with grating period as Λ_y) are parallel to POI, which can be considered as full conical mounting incidence, while the grating pillars along y-axis (with grating period as Λ_x) are normal to POI and can be considered as a classic mounting incidence. Therefore, the physical mechanism of the spectral responses of 2D GMRF can be analyzed in detail, in terms of the diffracted wave vectors of 1D GMRFs with classic and full conical mountings.

The wave vectors associated with m-th order diffraction of the 2D grating obey the following equations [30]:

$$\text{(Classic) } k_{x,m} = k_0 \sin\theta + m\left(\frac{2\pi}{\Lambda_x}\right) \quad k_{y,m} = 0, \tag{2}$$

$$\text{(Full conical)} \quad k_{x,m} = m\left(\frac{2\pi}{\Lambda_y}\right), \quad k_{y,m} = k_0 \sin\theta \tag{3}$$

where $k_{x,m}$ and $k_{y,m}$ represent the magnitudes of the components along x and y axes, respectively. $k_0 = 2\pi/\lambda$. Since the grating periods Λ_x and Λ_y of the 2D GMRF are sufficiently small compared to the incident wavelength, there are only zero-order diffractions ($m = \pm 1$).

The waveguide modes supported by the grating structure are leaky and thus its propagation constant is a complex number. And the real part of the propagation constant is related to the resonant location, which can be approximated by $\beta_m = (k_{x,m}^2 + k_{y,m})^{1/2}$ [31], [32]. Therefore, the propagation constants of the 2D GMRF with grating pillars along y-axis for $m = \pm 1$ orders are:

$$\beta_{\pm 1} = 2\pi\left(\frac{1}{\Lambda_x} \pm \frac{\sin\theta}{\lambda}\right) \tag{4}$$

For classic mounting, as shown in Eq. (4), as θ increases, the propagation constant with $m = -1$ decreases which result in redshifts with incident angle (branches I and V in Fig. 2), whereas the propagation constant with $m = 1$ increases which result in blueshifts with incident angle (branches II and VI in Fig. 2) [30].This is because the resonance wavelength is inversely proportional to $\beta_{\pm 1}$.

Whereas for grating pillars along x-axis, the propagation constant for $m = \pm 1$ orders, derived from Eq. (3), can be rewritten as:

$$\beta_{\pm 1} = 2\pi\sqrt{\left(\frac{\pm 1}{\Lambda_y}\right)^2 + \left(\frac{\sin\theta}{\lambda}\right)^2} \tag{5}$$

As for full conical mounting shown in Eq. (5), β_{+1} always equals to β_{-1} for oblique incidence, which means that the resonance bands of the 2D grating under full conical mounting are degenerate and they never split [29]. And this can explain the degenerate bands III and IV in Fig. 2.

According to the analysis of the physical mechanism of the spectral responses in 2D GMRF, the locations of the polarization independent resonances are mainly determined by the grating period along x-axis, since Λ_x is related to the split feature as shown in Eq. (4). Thus, adjusting the polarization-independent resonant location can be realized in terms of varying the grating period along x-axis (Λ_x).

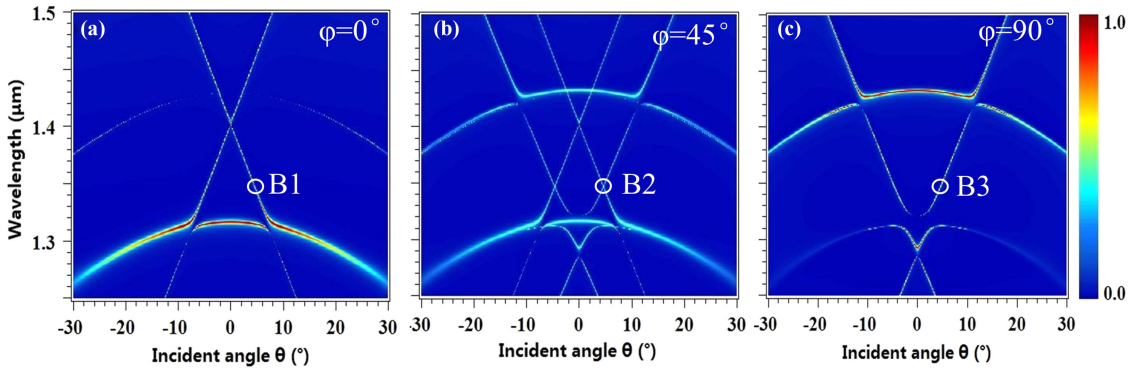

Fig. 4. Calculated results of angular-resolved reflectance (R_0) of the designed 2D filter with rectangular pillars ($\Lambda_x = 830$ nm, $\Lambda_y = 850$ nm) under three different polarization states. (a) $\varphi = 0°$ (S-polarization); (b) $\varphi = 45°$; (c) $\varphi = 90°$ (P-polarization).

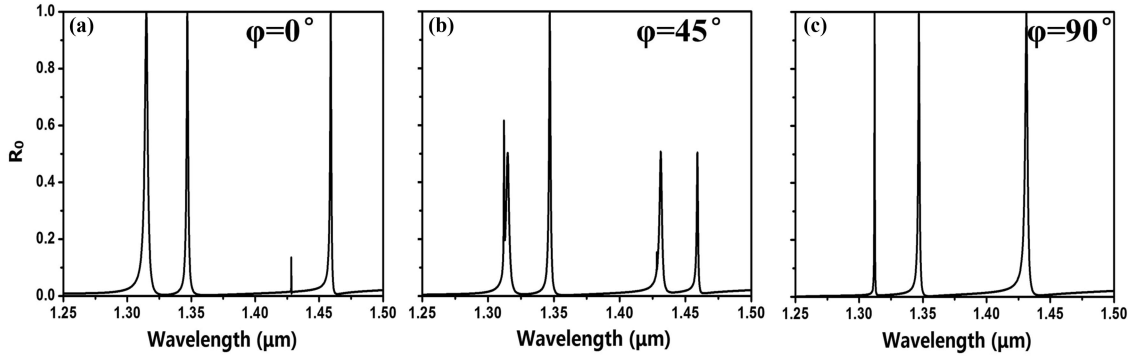

Fig. 5. Reflectance spectra of the designed 2D GMRF with rectangular pillars ($\Lambda_x = 830$ nm, $\Lambda_y = 850$ nm) under oblique incidence $\theta = 4.6°$ with three different polarization angles: (a) $\varphi = 0°$; (b) $\varphi = 45°$; (c) $\varphi = 90°$.

Fig. 4 shows the calculated results of the designed 2D GMRF under three different polarization angles, in which the grating period along x-axis Λ_x is adjusted from the optimized value 850 nm to 830 nm. There exist no changes of the degenerate bands (branches III and IV) compared with the spectral responses in Fig. 2, since the grating period along y-axis Λ_y remains unchanged. Whereas, the resonant locations of the split branches shift to shorter wavelengths, as shown in Fig. 4. Similarly, varying φ from 0° to 90° generates a continuously diffraction efficiency transition from Fig. 4(a) to 4(c). During the continuously transition, there is a distinct crossing point labeled B2 (4.6, 1.3569), which can be easily obtained from Fig. 4(b). The resonant wavelength is 1.3569 μm under oblique incidence with $\theta = 4.6°$. Besides, coordinate (4.6, 1.3569) also exists in Figs. 4(a) and 4(c) which marched as B1 and B3, respectively. Therefore, (4.6, 1.3569) is the polarization independent point that we are looking for.

In order to better understand the polarization insensitivity, reflectance spectra of the designed 2D GMRF with rectangular pillars ($\Lambda_x = 830$ nm, $\Lambda_y = 850$ nm) under oblique incidence $\theta = 4.6°$ are analyzed in Fig. 5, where three different polarization states (0°, 45° and 90°) are taken into consideration. Results show that the resonant location with wavelength 1.3569 μm is proved to be insensitive to polarization under oblique incidence of 4.6°, and the reflectance spectrum of the polarization-insensitive wavelength exhibits high diffraction efficiency, narrow band and low sideband, etc.

Increasing the grating period along x-axis Λ_x from the designed value 850 nm to 870 nm, and keeping the grating period along y-axis Λ_y unchanged, the polarization-independent location will shift to longer wavelength. And in order to clarify the conclusion, results about the angular-resolved

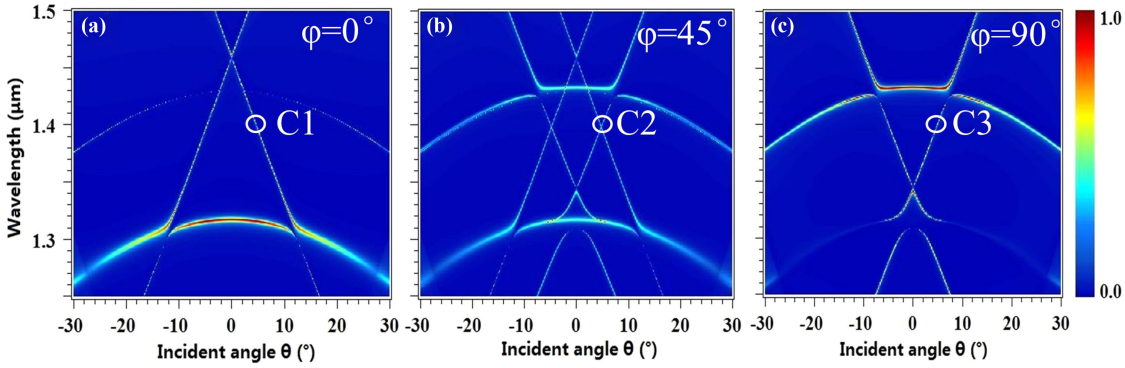

Fig. 6. Calculated results of angular-resolved reflectance (R_0) of the designed 2D filter with rectangular pillars ($\Lambda_x = 870$ nm, $\Lambda_y = 850$ nm) under three different polarization states. (a) $\varphi = 0°$ (S-polarization); (b) $\varphi = 45°$; (c) $\varphi = 90°$ (P-polarization).

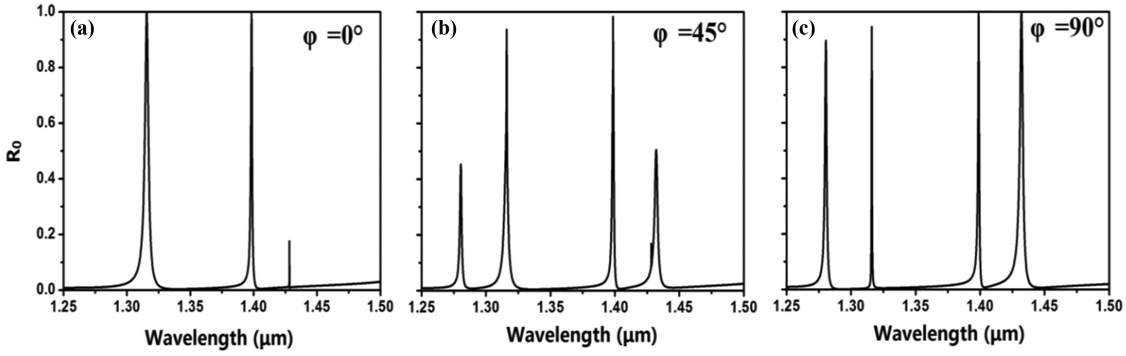

Fig. 7. Reflectance spectra of the 2D GMRF with rectangular pillars ($\Lambda_x = 870$ nm, $\Lambda_y = 850$ nm) under oblique incidence $\theta = 4.8°$ with three different polarization angles. (a) $\varphi = 0°$; (b) $\varphi = 45°$; (c) $\varphi = 90°$.

reflectance (R_0) of the designed 2D filter with rectangular pillars ($\Lambda_x = 870$ nm, $\Lambda_y = 850$ nm) under three different polarization states ($\varphi = 0°, 45°, 90°$) are illustrated in Fig. 6. There is a distinct crossing point C2 (4.8, 1.3985) between the split branches, which is obtained under $\varphi = 45°$ as shown in Fig. 6(b). Besides, coordinate (4.8, 1.3985) also exists in Figs. 6(a) and 6(c) which marched as C1 and C3, respectively. Therefore, a polarization independent location with wavelength 1398.5 nm appears as an oblique incidence with $\theta = 4.8°$ irradiates on the surface of 2D GMRF structure.

In order to prove the polarization-independence of the resonant location with wavelength 1398.5 nm, the reflectance spectra of the 2D GMRF with rectangular pillars ($\Lambda_x = 870$ nm, $\Lambda_y = 850$ nm) under oblique incidence $\theta = 4.8°$ are shown Fig. 7, where three different polarization angles are considered. The resonant location with wavelength 1398.5 nm are polarization insensitive as supposed.

As for POI in yz-plane, the spectral responses as well as the polarization-independent wavelength are consistent with those for POI in xz-plane due to the structural symmetry. While for POI between xz- and yz-plane, the grating pillars along x-axis as well as the grating pillars along y-axis are no longer parallel or perpendicular to POI. Take an azimuthal angle being 30° for example (here the azimuthal angle is defined as the angle between xz-plane and the POI), the calculated results of angular-dependent reflectance under are shown in Fig. 8. There are four pairs of split branches of the 2D GMRF as shown in Fig. 8. And varying the polarization angle generates a diffracton efficiency transition between the four pairs branches, which results into two crossed points *p*1 (5.4, 1.3731) and *p*2 (9.7, 1.3654) in the angular-dependent reflectance (R_0). The coordinates of the two crossed points correspond to the angles of oblique incidence and polarization-independent resonant locations. Fig. 9 shows the reflectance spectra of the 2D GMRF with azimuthal angle

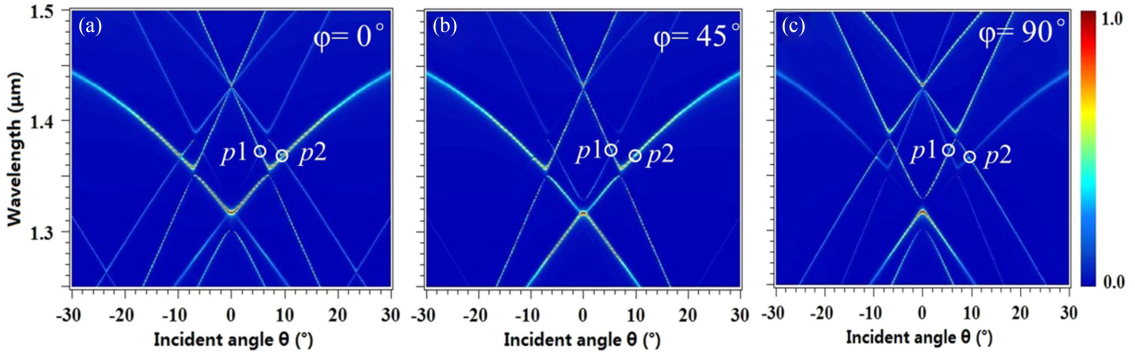

Fig. 8. Calculated results of angular-resolved reflectance (R_0) of the designed 2D filter with square pillars ($\Lambda_x = \Lambda_y = 850$ nm) with POI between xz- and yz-plane (the azimuthal angle is 30°). (a) $\varphi = 0°$; (b) $\varphi = 45°$; (c) (a) $\varphi = 90°$.

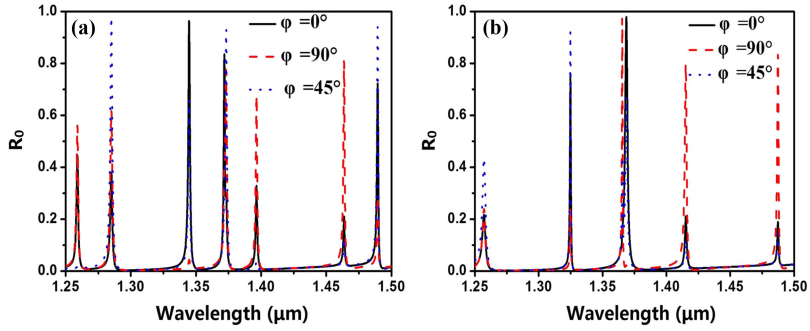

Fig. 9. Reflectance spectra of the designed 2D GMRF with square pillars ($\Lambda_x = \Lambda_y = 850$ nm) with POI between xz- and yz-plane (the azimuthal angle is 30°) under oblique incidences. (a) $\theta = 5.4°$; (b) $\theta = 9.7°$.

being 30°, under oblique incidences $\theta = 5.4°$ (Fig. 9(a)) and $\theta = 9.7°$ (Fig. 9(b)). The resonant locations for three different polarization states ($\varphi = 0°$, 45°, 90°) are all 1373.1 nm and 1365.4 nm for oblique incidences $\theta = 5.4°$ and$\theta = 9.7°$, respectively, though there exist a little diffraction efficiency differences. Thus, the methods proposed in this paper can also be applied to search for the polarization-independent locations with POI in yz-plane as well as POI between xz- and yz-plane.

4. Conclusion

In summary, we propose a compact method to realize polarization-independent wavelengths based on 2D crossed grating under oblique incidence. Since in filtering optical devices, the normal incidence regime is usually avoided because it requires the use of beam separators and will yield a loss of efficiency. Plane of incidence is set to be in xz-plane and three different polarization angles (0°, 45°, 90°) are used to demonstrate the polarization-insensitivity. According to the analysis of the physical mechanism of the 2D GMRF, in terms of the wave vectors in 1D GMRF with classic and full conical mountings, realization of the polarization-insensitivity is due to the split features which are mainly determined by the grating period along x-axis. Results show that, the greater the period along x-axis is, the longer wavelength of the polarization-independent resonance will be. For example, the polarization-insensitive wavelength shifts from 1356.9 nm to 1398.5 nm as adjusting the grating period along x-axis from 830 nm to 870 nm. Moreover, the results and methods provided herein can also be applied to search for the polarization-insensitive resonances of the 2D grating with any planes of incidence.

References

[1] P. R. Harris, A. Ricciardi, T. Krauss, and A. D. Falco, "Optical guided mode resonance filter on a flexible substrate," *Opt. Exp.*, vol. 21, no. 1, pp. 1002–1007, Jan. 2013.

[2] K. Yamada *et al.*, "Flat-top narrowband filters enabled by guided-mode resonance in two-level waveguides," *Opt. Lett.*, vol. 42, no. 20, pp. 4127–4130, Oct. 2017.

[3] Y. K. Tu, M. Z. Tsai, I. C. Lee, I. C. Lee, H. Y. Hsu, and C. S. Huang, "Integration of a guided-mode resonance filter with microposts for in-cell protein detection," *Analyst*, vol. 141, pp. 4189–4195, 2016.

[4] Y. Long, Y. Li, L. Shen, W. Y. Liang, H. D. Deng, and H. T. Xu, "Dually guided-mode-resonant graphene perfect absorbers with narrow bandwidth for sensors," *J. Phys. D, Appl. Phys.*, vol. 49, no. 32, p. 32LT01, Jul. 2016.

[5] A. Mizutani, H. Kikuta, and K. Iwata, "Numerical study on an asymmetric guided-mode resonant grating with a Kerr medium for optical switching," *J. Opt. Soc. Amer. A*, vol. 22, no. 2, pp. 355–360, Feb. 2005.

[6] M. J. Uddin and R. Magnusson, "Highly efficient color filter array using resonant Si3N4 gratings," *Opt. Exp.*, vol. 21, no. 20, pp. 12495–12506, May 2013.

[7] W. Wang *et al.*, "Angle- and polarization-dependent spectral characteristics of circular grating filters," *Opt. Exp.*, vol. 24, no. 10, pp. 11033–11042, May 2016.

[8] J. M. Foley, S. M. Young, and J. D. Phillips, "Symmetry-protected mode coupling near normal incidence for narrow-band transmission filtering in a dielectric grating," *Phys. Rev. B*, vol. 89, no. 165111, pp. 1–9, 2014.

[9] Y. Qin, Y. Yu, J. Zou, and X. Zhang, "Silicon based polarization insensitive filter for WDM-PDM signal processing," *Opt. Exp.*, vol. 21, no. 22, pp. 25727–25733, Nov. 2013.

[10] J. Li *et al.*, "Direct laser writing of symmetry-broken spiral tapers for polarization-insensitive three-dimensional plasmonic focusing," *Laser Photon. Rev.*, vol. 8, no. 4, pp. 602–609, 2014.

[11] M. R. Saleem, D. Zheng, B. Bai, and J. Turunen, "Replicable one-dimensional non-polarizing guided mode resonance gratings under normal incidence," *Opt. Exp.*, vol. 20, no. 15, pp. 16974–16980, Jul. 2012.

[12] M. R. Saleem, S. Honkanen, and J. Turunen, "Non-polarizing single layer inorganic and double layer organic-inorganic one-dimensional guided mode resonance filters," *Proc. SPIE*, vol. 8613, no. 86130C, pp. 1–7, Mar. 2013.

[13] D. Lacour, G. Granet, and J. P. Plumey, "Polarization independence of a one-dimensional grating in conical mounting," *J. Opt. Soc. Amer. A*, vol. 20, no. 8, pp. 1546–1552, Aug. 2003.

[14] B. Xu, D. Zhang, Y. Wang, Y. Huang, and Q. Wang, "Design and characteristics of polarization-insensitive resonant gratings for color filtering," *J. Modern Opt.*, vol. 60, no. 21, pp. 1961–1966, 2013.

[15] G. Niederer, W. Nakagawa, and H. P. Herzig, "Design and characterization of a tunable polarization-independent resonant grating filter," *Opt. Exp.*, vol. 13, no. 6, pp. 2196–2200, Mar. 2005.

[16] H. X. Hui, G. Ke, S. T. Yu, and D. M. Wu, "Polarization-independent guided-mode resonance filters under oblique incidence," *Chin. Phys. Lett.*, vol. 27, no. 7, 2010, Art. no. 074211.

[17] X. M. Gao *et al.*, "Angular-dependent polarization-insensitive filter fashioned with zero-contrast grating," *Opt. Exp.*, vol. 23, no. 12, pp. 15235–15241, Jun. 2015.

[18] D. Y. Wang, Q. K. Wang, and D. M. Liu, "Polarization-insensitive filter for incidence between classic and full conical mountings," *IEEE Photon. Technol. Lett.*, vol. 30, no. 495, pp. 495–498, Mar. 2018.

[19] M. G. Moharam, "Coupled -wave analysis of two -dimensional dielectric gratings," *SPIE*, vol. 883, pp. 8–11, 1988.

[20] P. Song and G. M. Morris, "Resonant scattering from two-dimensional gratings," *J. Opt. Soc. Amer. A*, vol. 13, no. 5, pp. 993–1005, May 1996.

[21] D. W. Peters *et al.*, "Demonstration of polarization-independent resonant subwavelength grating filter arrays," *Opt. Lett.*, vol. 35, no. 19, pp. 3201–3203, Oct. 2010.

[22] A. J. Pung, M. K. Poutous, R. C. Rumpf, Z. A. Roth, and E. G. Johnson, "Two-dimensional guided mode resonance filters fabricated in a uniform low-index material system," *Opt. Lett.*, vol. 36, no. 16, pp. 3293–3295, Aug. 2011.

[23] A. L. Fehrembach and A. Sentenac, "Unpolarized narrow-band filtering with resonant gratings," *Appl. Phys. Lett.*, vol. 86, no. 121105, pp. 1–3, Mar. 2005.

[24] S. Hernandez *et al.*, "High performance bi-dimensional resonant grating filter at 850 nm under high oblique incidence of $\sim$60°," *Appl. Phys. Lett.*, vol. 92, no. 131112, pp. 1–3, Apr. 2008.

[25] A. L. Fehrembach, F. Lemarchand, A. Talneau, and A. Sentenac, "High Q polarization independent guided-mode resonance filter with "Doubly Periodic" etched $Ta2O_5$ bidimensional grating," *J. Lightw. Technol.*, vol. 28, no. 14, pp. 2037–2044, Jul. 2010.

[26] M. S. Saremi and R. Magnusson, "Properties of two-dimensional resonant reflectors with zero-contrast gratings," *Opt. Lett.*, vol. 39, no. 24, pp. 6958–6961, Dec. 2014.

[27] Q. Wang, Q. Liu, Y. Li, Y. S. Huang, and D. W. Zhang, "Characteristics of guided-mode resonance filter with elliptically polarized incident light," *IEEE Photon. J.*, vol. 9, no. 1, Feb. 2017, Art. no. 7800610.

[28] W. Wang *et al.*, "Polarization-insensitive concentric circular grating filters featuring a couple of resonant peaks," *IEEE Photon. J.*, vol. 7, no. 5, Oct. 2015, Art. no. 7102010.

[29] W. Wang, X. M. Gao, X. F. Shen, Z. Shi, and Y. J. Wang, "Spectral responses of linear grating filters under full-conical incidence," *Opt. Lett.*, vol. 43, no. 3, pp. 391–394, Feb. 2018.

[30] H. K. Yeong, N. Manoj, and R. Magnusson, "Divergence-tolerant resonant bandpass filters," *Opt. Lett.*, vol. 41, no. 14, pp. 3305–3308, Jul. 2016.

[31] R. Magnusson and S. S. Wang, "New principle for optical filters," *Appl. Phys. Lett.*, vol. 61, no. 9, pp. 1022–1024, Aug. 1992.

[32] S. S. Wang and R. Magnusson, "Theory and applications of guided-mode resonance filters," *Appl. Opt.*, vol. 32, no. 14, pp. 2606–2613, May. 1993.